Chapter 11

Analysis of a Resonant AC-AC LED Driver

Teodosescu Petre Dorel, Szekely Norbert Csaba,

Sabau Madalina Sabina and Bojan Mircea

Additional information is available at the end of the chapter

http://dx.doi.org/10.5772/67472

Abstract

The study analyses the performance of different LED circuit configurations feed from a low power resonant driver under pulse quasi-triangular currents. The considered LED driver topology is based on a bridgeless single-stage AC-AC converter with bidirectional switches and a parallel LC resonant tank. The converter performances are simultaneously analyzed in correlation with the most important features, such as the electric efficiency, luminous efficacy, power factor correction capabilities, and flickering implications.

Keywords: light-emitting diodes, converters, resonant conversion, soft switching

1. Introduction

Nowadays, once with the improvements in process and technology, light-emitting diodes (LEDs) have become a very popular solution for lighting devices due to its superior efficacy performance. It is well known that many electronic converters are using an input rectifier and a high-electrolytic filtering capacitance [1, 2]. In high frequency commutations, this electrolytic capacitors have reliability issues, and this fact is limiting the lifetime of the overall LED system [3–7]. In addition, the use of high capacitance electrolytic capacitors remains a problem in achieving high power density and high power factor. Refs. [8–11] propose different topologies of AC-DC converters capable to increase the lifetime of LED driver, by using film capacitors instead of electrolytic capacitors. The basic idea of Ref. [8] is to increase the conduction time of the input current consuming more at the peak and less at the valley of the input power. A high power factor LED driver topology consisting of a derivate topology from a two-cascade flyback converter is presented in Ref. [9]. Thus, the proposed single-stage, single-switch topology is able to provide high power factor without any unreliable electrolytic capacitors. Moreover, no feed-back control circuit is required for minimizing the low-frequency ripple of the LED current. Ref. [10] proposes an AC/DC driver, which is able to provide constant current for LEDs and near-unity input power factor, as well. The idea of this chapter consists in modulating the input current, using pulsating current to drive LEDs and some energy storage elements to balance the power difference. Bearing in mind all these, it is unanimously accepted that in order to increase the lifespan of artificial LED lighting, the elimination of electrolytic capacitors is a must. Like-wise, the need to increase the power factor of this electronic load together with constant output current is necessary measures for sustainable development of these technologies [12, 13].

For AC-DC LED drivers, light flicker introduced by the low-frequency pulsating current represents a real problem for the performance of the system and can also have negative influence on human vision [14]. Ref. [15] presents a series-resonant converter (SRC), which can be used as a power control stage able to reduce the low-frequency ripple of the LED current. Additionally, a good performance of the system is gained due to the low switching losses of the SRC and by using film capacitors instead of electrolytic capacitance at the output of power factor correction (PFC) stage. Ref. [16] offers another method capable to obtain a low current ripple by using an average current modulator in series with the LED load. In Ref. [17], a flicker-free electrolytic capacitor-less single-phase AC-DC LED driver is being introduced. By using a bidirectional buck-boost converter, the topology is capable to limit the AC component of the pulsating current and let only the DC component to drive the LEDs. The idea of obtaining an output low-current ripple for avoiding flicker problem is also found in Ref. [18]. This work offers a two-stage flyback/Buck converter topology for which a low output current ripple is obtained. Taking into account all the facts mentioned above, many research interests are related to the minimization of the low-frequency current ripples first because of optical behavior and lifespan of the LED and second because of the lower efficacy of LED in high current ripples [19]. Given that, a low ripple for the LED current can be considered a good practice in designing of high quality LED lighting systems.

In some situations, such as direct AC LED lighting devices [20–22], the high current ripples prove not to be a problem at frequencies of 100 Hz or higher. At these frequencies, the light flicker is considered invisible for most people as is presented in [23–25]. A negative impact for human vision is the stroboscopic effect from flicker, which can be permanently avoided at frequencies higher than 300 Hz.

The present work introduces a new AC-AC resonant converter topology, wherein the main novelty consists on directly feeding from mains a resonant LC tank by two bidirectional switches. In comparison with Ref. [26], the advantage is the elimination of the input diode rectifier, which mainly is translated into achieving higher efficiency. Also, the driver topology is characterized by inherent constant current and high power factor; thus, no close-loop control is considered. The results are presented in correlation with: the electric efficiency, luminous efficacy, power factor correction capabilities, and flicker parameters implications.

The study is organized with a nomenclature section followed by an introduction. Section 3 analytically analyzes the proposed topology and its working principles, while Section 4 deals in the practical measurements of the proposed topology. Section 5 is dedicated for the conclusion, and some hints on future work to be done for further improvements are provided.

http://dx.doi.org/10.5772/67472

2. Considered LED driver topology

In this section, the considered LED driver topology is introduced. The circuit is subject to a patent application [27] and is based on an AC-AC quasi-resonant LC parallel converter driving an output LED stage. The considered topology is presented in **Figure 1**.

It can be seen in **Figure 1** that the AC-AC converter is composed of two bidirectional switches, each having two MOSFETs connected with a common source. In this way, the transistors' control signals can be easily obtained from an IC (in this case, an IR21531 was used) or discrete self-oscillating driver. Using only two signals to control all four transistors is advantageous due to the simplicity and cost-related implications. In **Figure 2**, the presumptive waveforms of the main signals are displayed. From the upper part of the image, it can be seen that the transistors' command signals are represented by 50% duty-cycle signals.

In **Figures 3** and **4** for the input positive and negative half-cycles, the main circuit states depicting the current paths and the activated switches are highlighted. It can be noted that six different stages can be found on both the positive and negative input half-cycles, as presented in **Figure 2**.

Referring to **Figure 1**, the resulted simplified circuit is exemplified in **Figure 5**. The transistors T1 and T2 are represented by the bidirectional switch S1, while T3 and T4 by the bidirectional switch S2.

The analysis is made by considering the positive cycle of the input alternative voltage. Starting from the simplified converter model in **Figure 5**, from the presumptive waveforms in **Figure 2**, and the current paths in **Figure 3**, not considering the switching time frames, three main time intervals can be identified for a half-cycle:

(a) For the time interval defined in **Figure 2** between $t0$ and $t1$, corresponding to **Figure 3** state I, the switch S1 is conductive and S2 is in the OFF state, the converter equation is:

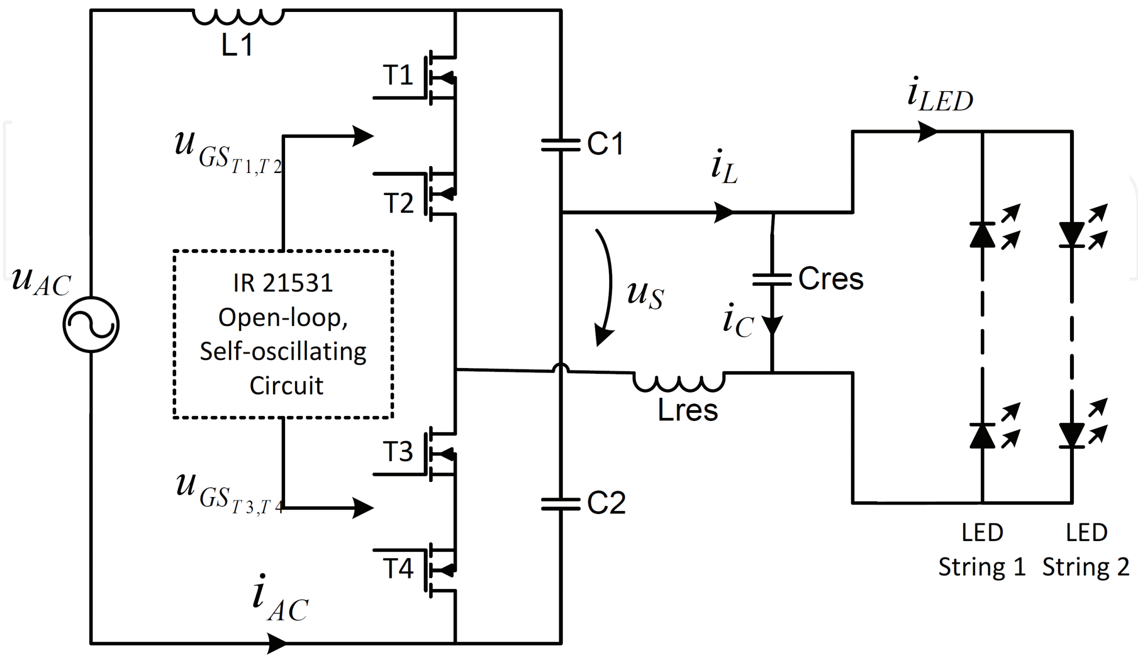

Figure 1. Considered LED driver.

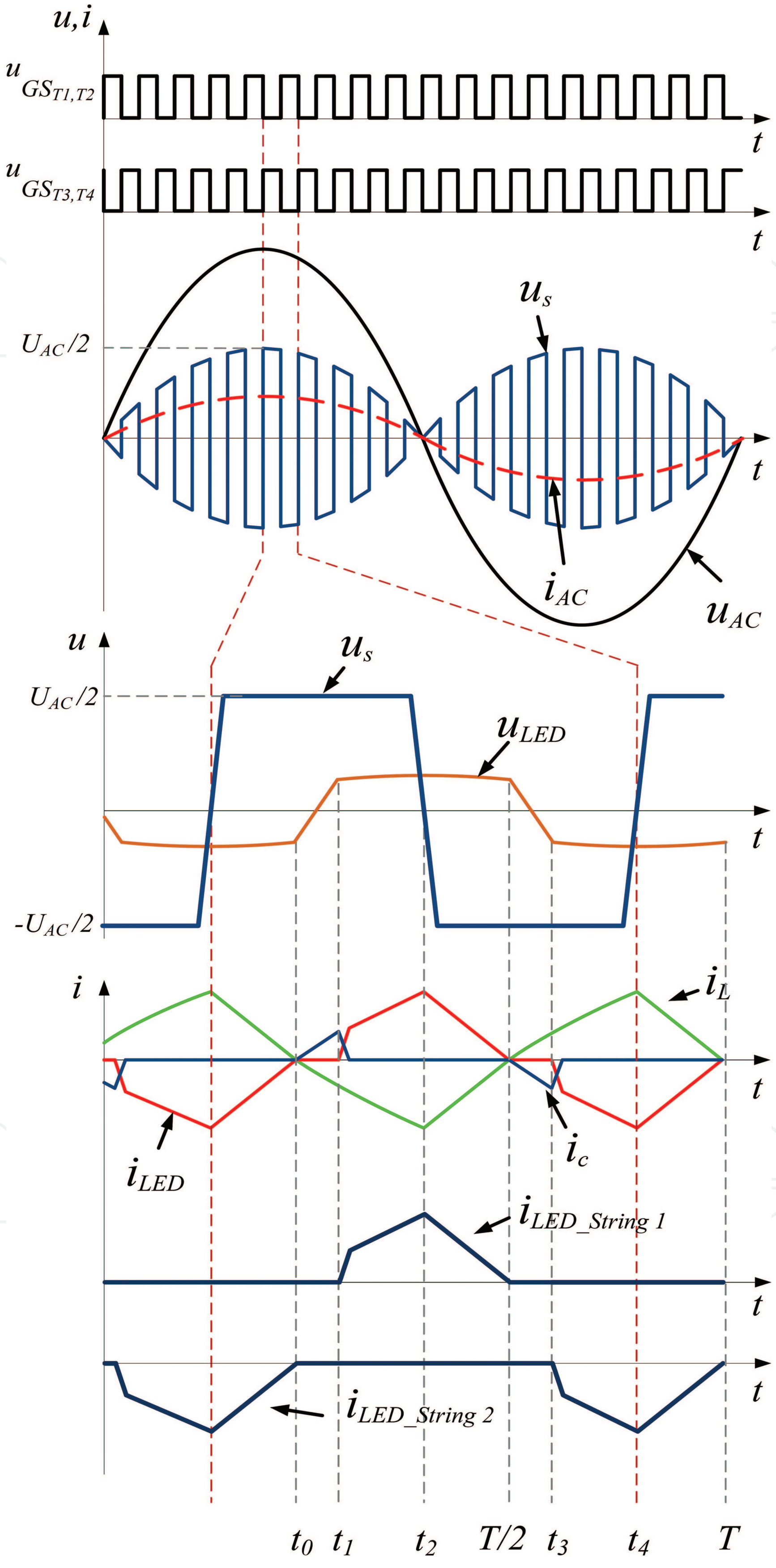

Figure 2. Presumptive waveforms of the AC-AC LED driver.

$$u_s(t) = L_{\text{RES}} \frac{di_L(t)}{d(t)} + u_{\text{LED}}(t) \tag{1}$$

Now, the circuit is in resonant mode, with no current in the LED ($i_{\text{LED}}(t) = 0$):

$$u_c(t) = \frac{1}{C_{\text{RES}}} \int i_c(t)dt \tag{2}$$

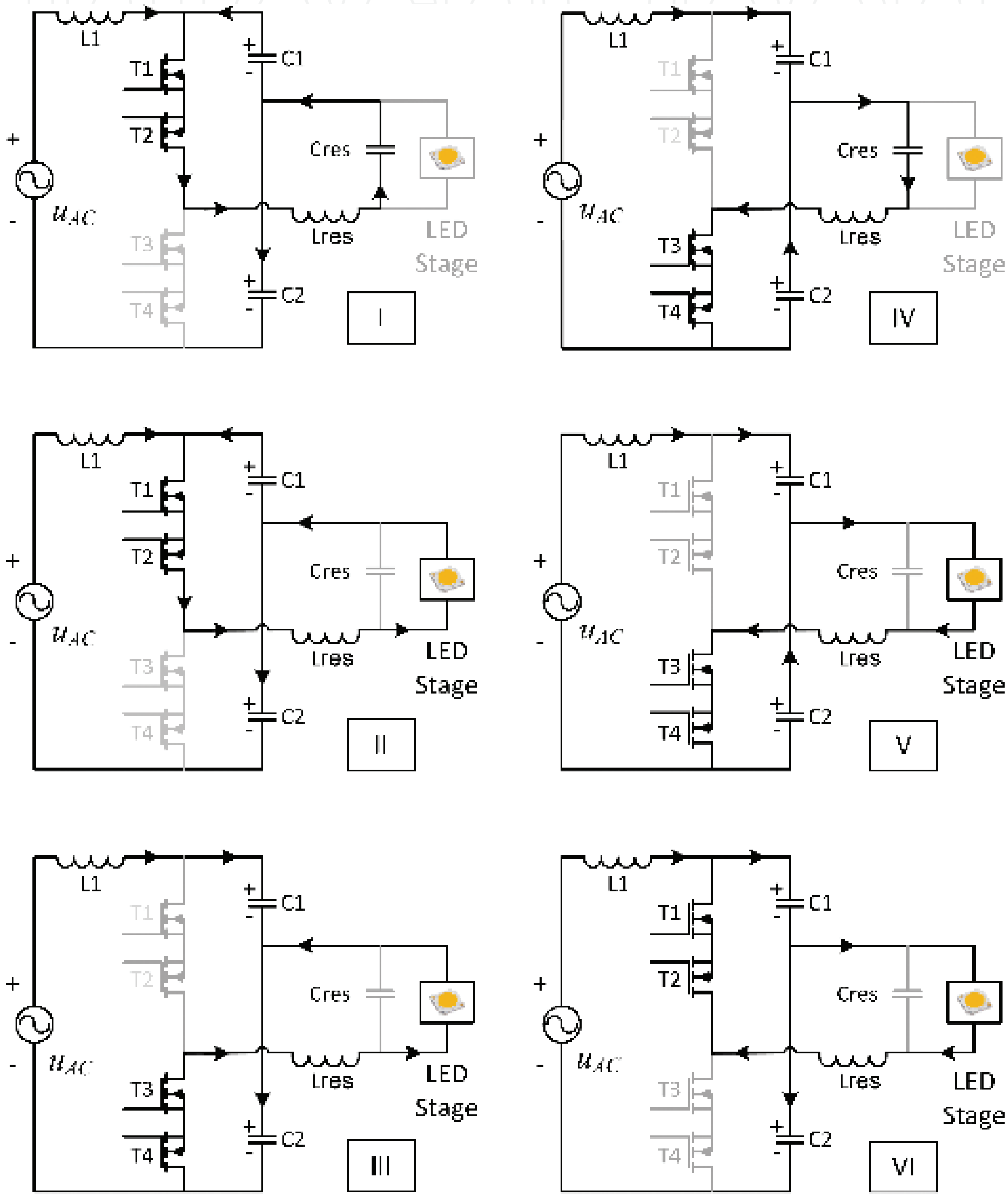

Figure 3. The six main time intervals for the input positive half-cycle.

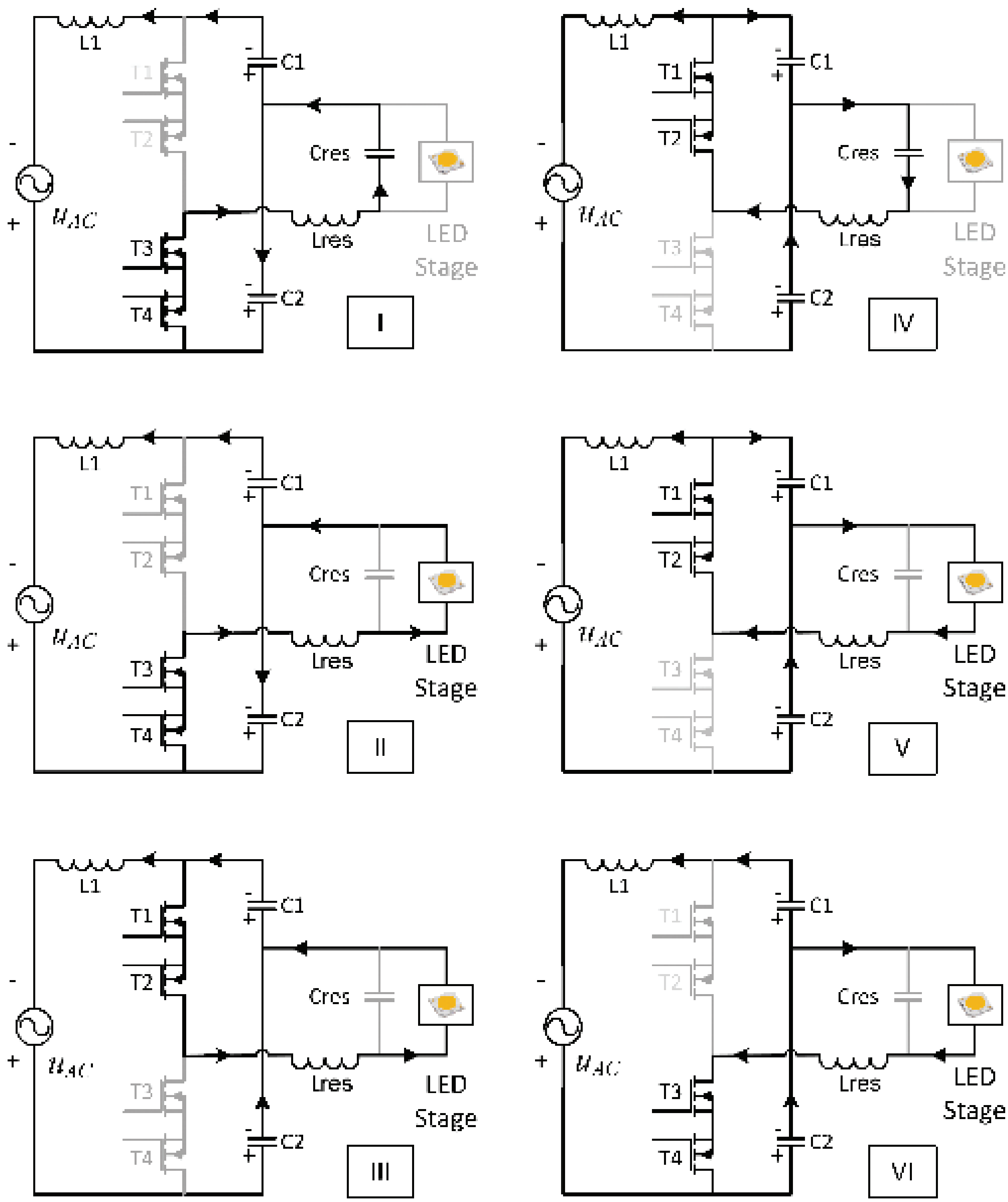

Figure 4. The six main time intervals for the input negative half-cycle.

For this time interval, the inductor current is equal to the capacitor current:

$$i_L(t) = i_C(t) \tag{3}$$

(b) For the time interval between t_1 and t_2, corresponding to **Figure 3**, state II, same as for previous interval, the switch S1 is in the ON state and the switch S2 in the OFF state:

http://dx.doi.org/10.5772/67472

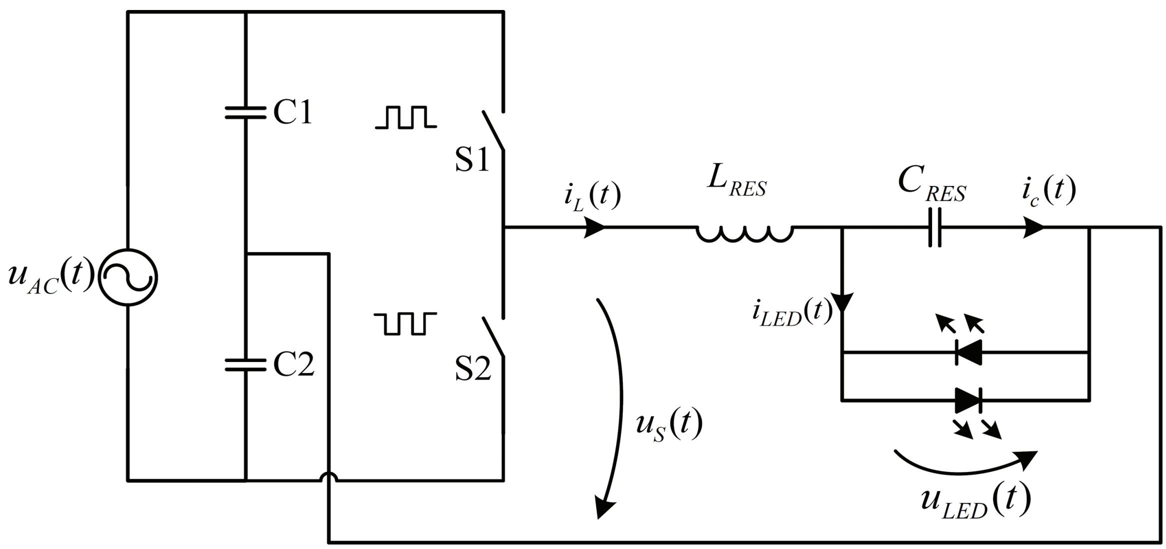

Figure 5. Simplified, model-based schematics of the consider LED driver.

$$u_s(t) = L_{\text{RES}} \frac{di_L(t)}{d(t)} + u_{\text{LED}}(t) \tag{4}$$

Now, $u_{\text{LED}}(t) > U_{\text{LED}}$ (the forward voltage of the direct biased LED), and for the considered time frame where $u_s(t) = \frac{U_{\text{AC}}}{2}$, the above equation becomes:

$$\frac{di_L(t)}{d(t)} = \frac{\frac{U_{\text{AC}}}{2} - U_{\text{LED}}}{L_{\text{RES}}} \approx \text{const.} \tag{5}$$

Because the direct biased LED is conductive, the capacitor current equals 0; thus, the coil current is equal to the LED current, as in:

$$i_L(t) = i_{\text{LED}}(t) \tag{6}$$

(c) For the time interval between t_2 and $T/2$, corresponding to **Figure 3**, state III, the switch S1 is in OFF state and the switch S2 is in ON state, the converter equation becomes:

$$-u_s(t) = L_{\text{RES}} \frac{di_L(t)}{d(t)} + u_{\text{LED}}(t) \tag{7}$$

In this time interval, $u_{\text{LED}}(t) > U_{\text{LED}}$, thus:

$$-\frac{di_L(t)}{d(t)} = \frac{\frac{U_{\text{AC}}}{2} - U_{\text{LED}}}{L_{\text{RES}}} \approx \text{const.} \tag{8}$$

Because the direct biased LED is still in conductive mode, the inductor current is equal to the LED current:

$$i_L(t) = i_{\text{LED}}(t) \tag{9}$$

At the time $t = T/2$, the direct biased LED current reaches the 0 value, and from this moment, the above presented behavior is being repeated for the remaining half cycle. As can be seen in **Figure 4**, the same behavior can be found during the negative cycle of the mains voltage.

It is known that the forward voltage of the LED changes with temperature, so in view of this:

$$-\frac{di_L(t)}{d(t)} = \frac{\frac{U_{AC}}{2} + U_{LED} \pm u_{LED}(^{\circ}C)}{L_{RES}} \tag{10}$$

One can admit that $u_{LED}(^{\circ}C) \ll \frac{U_{AC}}{2} + U_{LED}$, thus:

$$-i_{LED}(t) = \frac{\frac{U_{AC}}{2} + U_{LED} \pm u_{LED}(^{\circ}C)}{L_{RES}} \approx \text{const.} \tag{11}$$

Consequently, the proposed schematic has a current source behavior, with constant output current, regardless of the output LED load type/characteristics. From the input point of view, the circuit presents, to some extent, a natural corrective power factor function.

In **Figures 6** and **7**, the simulation results obtained with PSim 10 software point out the high power factor attained by the proposed circuit. The mains input current waveform for half a cycle is slightly liner/constant and, admittedly, the input current waveform shows, once more, the current source/constant current behavior of the converter.

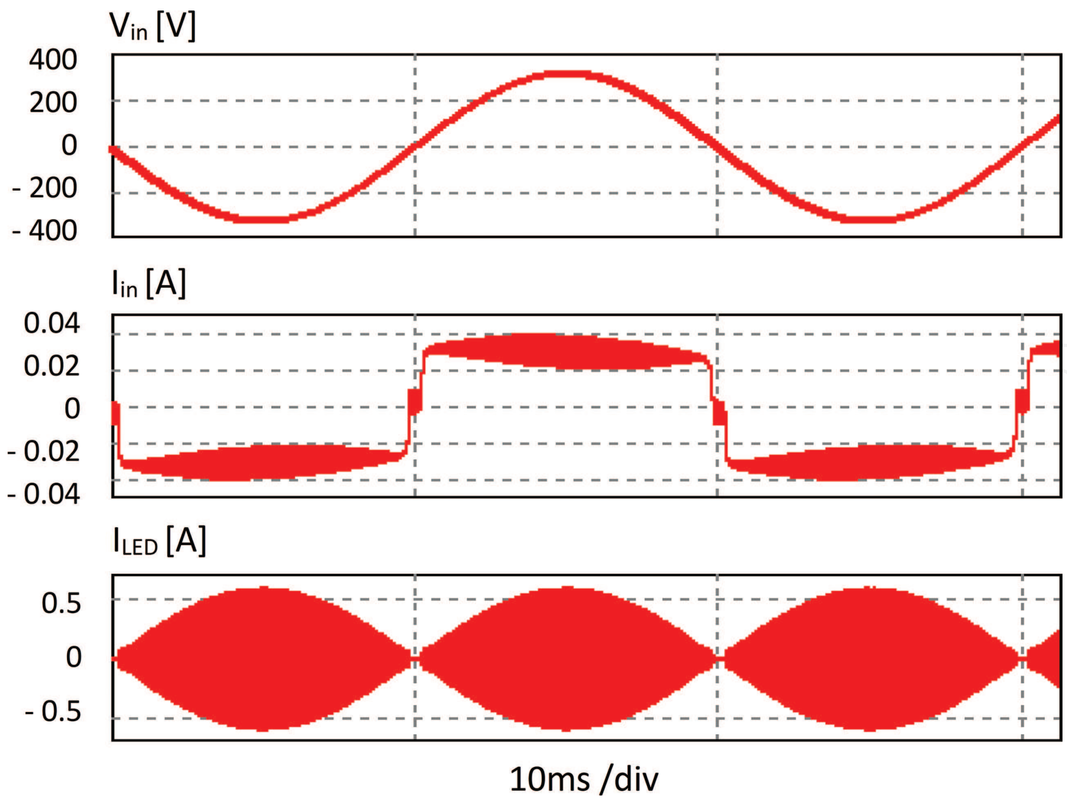

Figure 6. Simulated low frequency representation of the input voltage/current and output current i_{LED}.

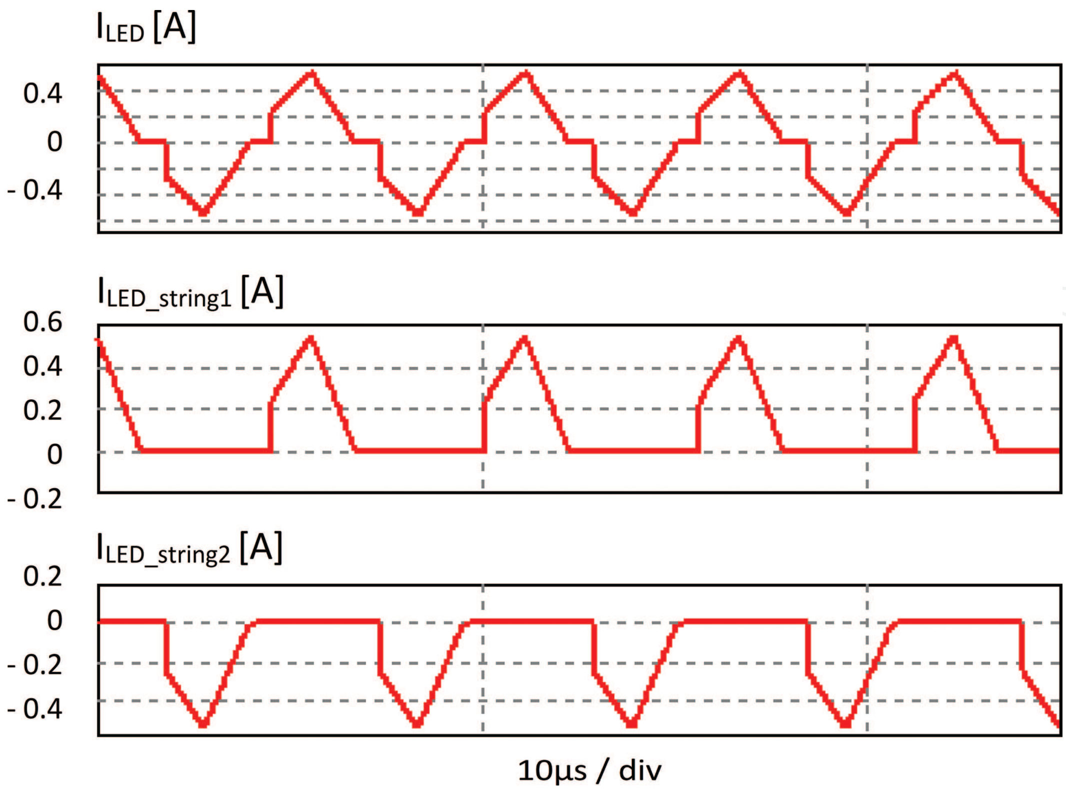

Figure 7. Simulated high frequency representation of the output current waveforms: output resonant tank current; LED string 1 current; LED string 2 current.

3. Practical implementation of the AC-AC LED driver

The practical measurements have been done on the converter topology from **Figure 1** (named the AC-AC type) using the following LED modules: CREE- XLamp CXA1304, CITIZEN-CLU028-1202C4-40AL7K3, and OPTOFLASH-OF-LM002-5B380. Because the Cree LED has an antiparallel diode, the circuit from **Figure 8**, named the AC-AC-1 type, is proposed where a fast diode, with low voltage drop, has been introduced in series with each LED strings.

General characteristics and converter components used are: IR21531 self-oscillating IC, IRF640 transistors, STPS2L40 high-frequency diode, L_{RES} – 2 mH resonant coil, C_{RES} – 2.2 nF resonant capacitor, C1-C2 100 nF voltage divider, L1 – 4 mH input filter, and 82 kHz switching frequency.

To reinforce the presumptive waveforms from **Figure 2**, the experimental results for the direct AC-AC driver considering the Citizen LED module are shown in **Figures 9–12**, wherein the signals are being presented both at low and high frequency ranges.

On the upper part of **Figure 9**, the input voltage $u_{AC}(t)$ and current $i_{AC}(t)$ are represented. On the lower part, the low frequency representation of the output resonant tank voltage, $u_s(t)$ and LED current, $i_{LED}(t)$ is highlighted. **Figure 10** presents the main output signals in relation with the transistor control signal $u_{GS,\ T1,\ T2}$. Therefore, the output voltage of the resonant tank, $u_s(t)$ is represented in conjunction with the LED voltage, $u_{LED}(t)$ and LED current, $i_{LED}(t)$.

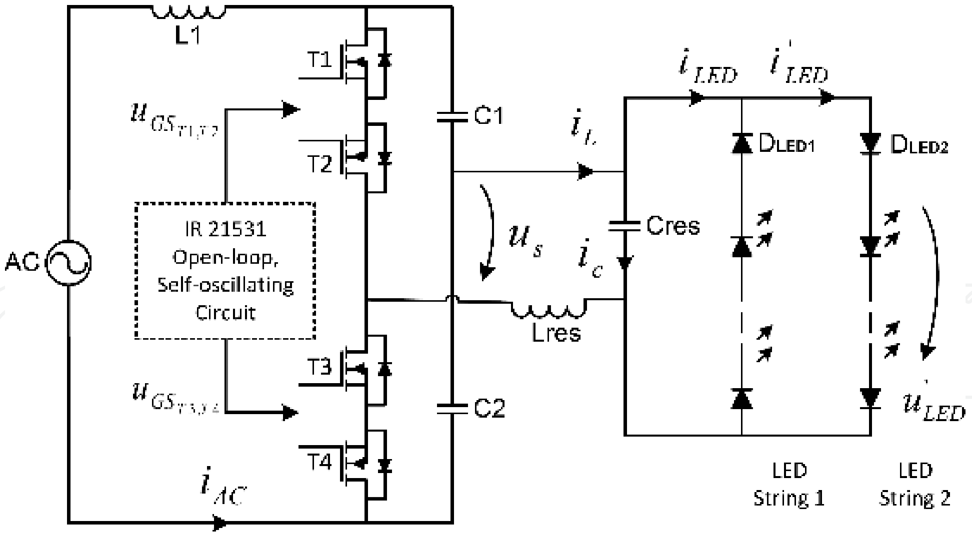

Figure 8. Proposed AC-AC-1 type converter.

Figure 11 highlights the voltage at the drains for the bidirectional switch composed of T1 and T2 transistors in conjunction with the gate control signals and the output LED current. One can notice that the gate signal used for the T1 and T2 transistors is applied after the voltage at the drains was lowered close to zero, thus ZVS (zero voltage switching) is attained. This represents one of the most important aspects in using resonant converters, where the switching losses are

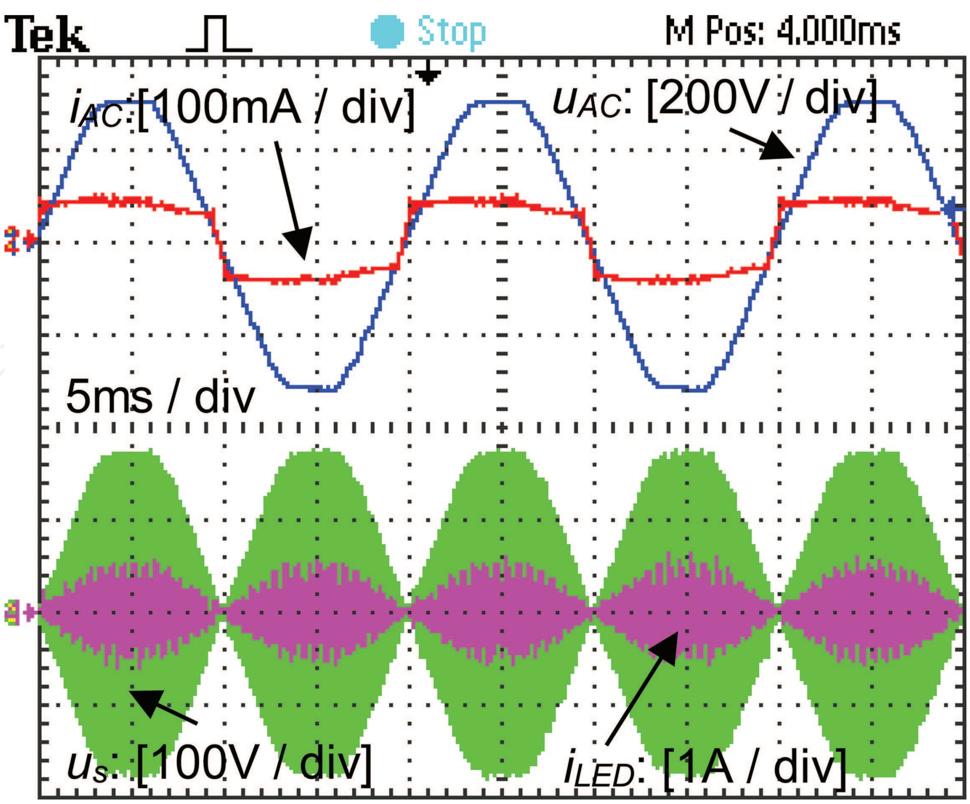

Figure 9. Low frequency signals representation: the input voltage $u_{AC}(t)$; the current $i_{AC}(t)$; the output resonant tank voltage, $u_s(t)$; the LED current, $i_{LED}(t)$.

http://dx.doi.org/10.5772/67472

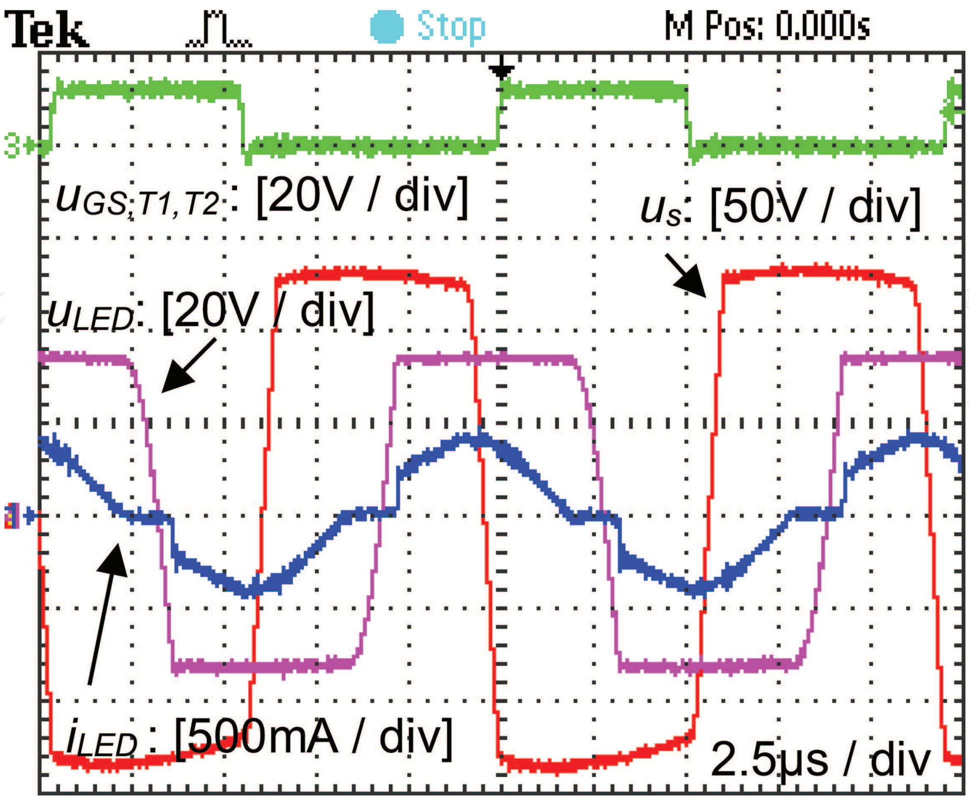

Figure 10. High frequency signals representation: transistor control signal $u_{GS,\ T1,\ T2}$;. The output voltage of the resonant tank, $u_s(t)$; LED voltage, $u_{LED}(t)$; LED current, $i_{LED}(t)$.

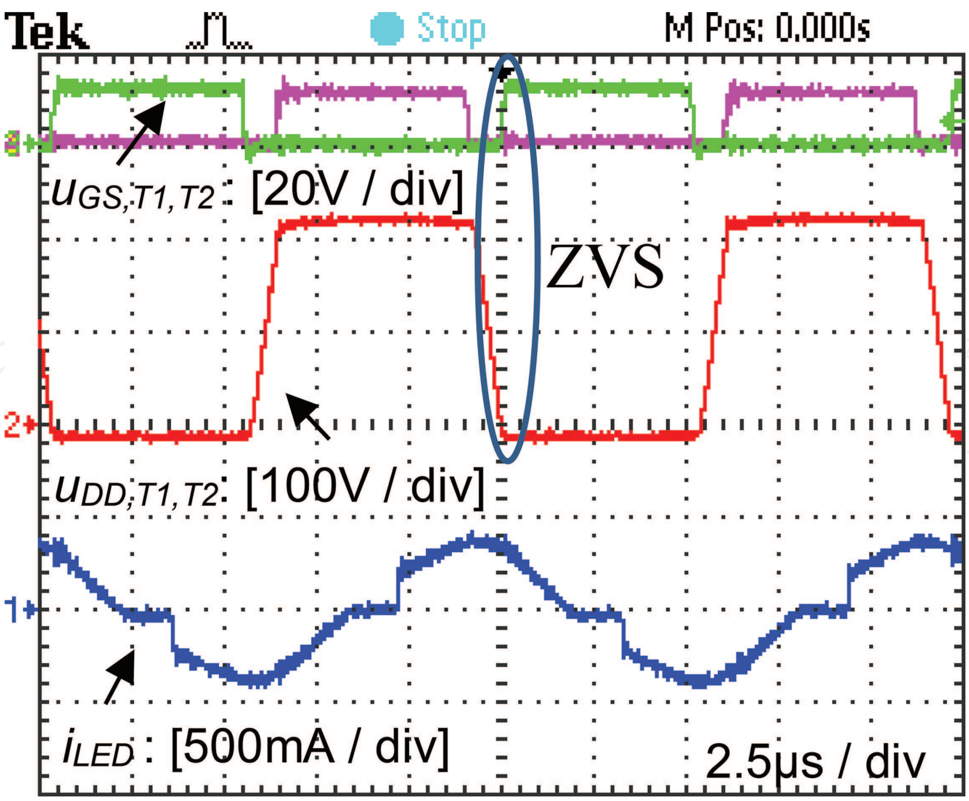

Figure 11. High frequency signals representation: the gate control signals (upper part); the voltage at the drains for the T1-T2 bidirectional switch; the output LED current (lower part).

narrowed to a minimum value. Moreover, the ZVS helps limiting the EMI levels caused by high-frequency switching converters.

Figure 12 shows, on the upper part, the output current of the resonant tank composed of the LED current, $i_{\mathrm{LED}}(t)$, and the resonant capacitor current, $i_C(t)$. On the lower part of the picture, the LED String 1 current and the LED String 2 current are being represented.

The general performances of the converter with all the three LED modules are centralized in: **Table 1** for the Cree LED, **Table 2** for Citizen LED, and **Table 3** for the OptoFlash LED. The power measurements were completed by the use of the precision power analyzer KinetiQ PPA2530. The flicker measurements have been performed with the light sensor OPT101 from Texas Instruments. From these waveforms, the percent flicker and the flicker index were deducted.

For all the LED types, the converter components and the switching frequency were kept the same, and since the forward voltage of the modules was different, dissimilar input power values have been obtained. Analyzing the electric efficiency, it can be observed that higher efficiency is achieved at higher input power, regardless of the LED type used. Also, the power factor is negatively influenced by the lower input power level.

The implementation of control loops was not an objective of the present study. Thus, the study states that for low power, acceptable performances in terms of light quality, high efficacy, and long lifespan with no capacitive filtering, the single-stage AC-AC with two antiparallel LED

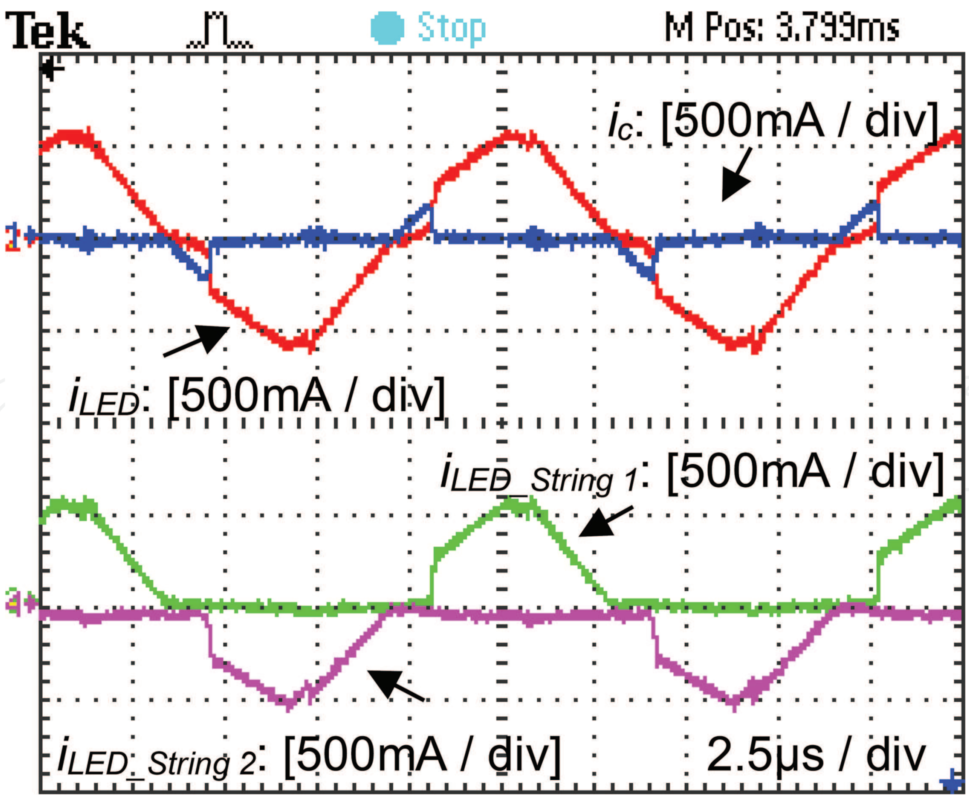

Figure 12. High frequency signals representation: the LED current, $i_{\mathrm{LED}}(t)$ and the resonant capacitor current, $i_C(t)$ (upper part); LED String 1 current and the LED String 2 current (lower part).

	Input power [W]	Electric efficiency [%]	System efficacy [lm/W]	Power factor	THD [%]	Flicker index	Percent flicker [%]
AC-AC	–	–	–	–	–	–	–
AC-AC-1	5.03	79.6	102.39	0.916	28.0	0.35	100

Table 1. Practical measurements—LED-Cree.

	Input power [W]	Electric efficiency [%]	System efficacy [lm/W]	Power factor	THD [%]	Flicker index	Percent flicker [%]
AC-AC	7.9	91	134.36	0.95	29.8	0.3	100
AC-AC-1	7.97	90.3	128.68	0.952	29.1	0.30	100

Table 2. Practical measurements—LED-Citizen.

	Input power [W]	Electric efficiency [%]	System efficacy [lm/W]	Power factor	THD [%]	Flicker index	Percent flicker [%]
AC-AC	7.15	89.7	97.45	0.952	28.8	0.34	100
AC-AC-1	7.24	88.2	96.91	0.926	29	0.34	100

Table 3. Practical measurements—LED-Optoflash.

strings could be an interesting solution. For upgraded results, mainly related with light quality, output rectifying solutions with high capacitance filtering are solutions to be investigated. The inherent current source behavior of the converter and high power factor are naturally being accomplished. For further improvements, pure sinusoidal input current shape building and dimming functions can be implemented by means of variable frequency closed-loop control.

The proposed solution was closely analyzed, considering most of the known issues and good practices. The need for high power factor together with constant output current is the feature of an LED drive that is not the subject of discussion. Also, high efficacy, light quality, and lifespans in a cost-efficient technology are targets for high performance LED devices. The study attempts to address all aspects presented above, but as a well-known general rule, some of the above criteria are more important than others, which are defined by the target application.

4. Conclusion

The present research introduces a method of using the benefits of soft switching, by the implementation of a resonant converter in controlling the current for LED lighting devices. The topology is a single-stage AC-AC converter that is capable of obtaining high power factor in an inherent way, with no feedback control loop. What is more, the circuit has a strong current source behavior; thus, no imperative constant output current control is required. All the characteristics are inherently attained, with no control loops; thus, there is room left for further improvement.

Mainly related with the AC-AC stage, the feasibility of the suggested solution is increased if electronic components manufacturing companies are willing to introduce bidirectional controlled switches in a single-chip technology for all power/voltage range applications.

Future work can consider the output circuits with low or high capacitance filtering, closed loop constant current controls, discrete self-oscillating control circuit, and higher switching frequencies for lower inductance needed for the resonant coil.

Acknowledgements

This work was supported by a grant from the Romanian National Authority for Scientific Research, MEN-UEFISCDI, project PN-II-PT-PCCA-2013-4-0914, No. 60/2014 - in the frame of the project with the title"Innovative electric power grid protection device against low power factor electronic loads" (IEDPFC).

Nomenclature

C_{RES}	Resonant tank capacitor
D	Duty cycle; diode
i_{LED}	Input current for the LED arrangement circuit
i_{AC}	Alternative input current
i_C	Resonant tank capacitor current
i_L	Resonant tank inductor current
L_{RES}	Resonant tank inductor
S_n	Bidirectional switch n
t	Time
u_{AC}	Alternative input voltage
$u_{DD,T1,T2}$	Drains voltage for the T1-T2 bidirectional switch
u_{GS}	Gate-source control voltage
u_{LED}	LED voltage
U_{LED}	LED forward voltage
u_S	AC-AC converter output voltage

Author details

Teodosescu Petre Dorel*, Szekely Norbert Csaba, Sabau Madalina Sabina and Bojan Mircea

*Address all correspondence to: petre.teodosescu@emd.utcluj.ro

Technical University of Cluj-Napoca, Cluj-Napoca, Romania

References

[1] J. W. Yang and H. L. Do. High-efficiency ZVS AC-DC LED driver using a self-driven synchronous rectifier. IEEE Transactions on Circuits and Systems: Regular Papers. 2014;**61**(8):2505–2512. DOI: 10.1109/TCSI.2014.2309837

[2] C. Cheng, C. H. Chang, F. Yang and T. Chung. A novel single-stage high-power-factor LED driver for street-lighting applications. IEEE Power Electronics and Drive Systems. 2013;**IA-21**:330–333. DOI: 10.1109/PEDS.2013.6527039

[3] J. M. Alonso, D. Gacio, A. J. Calleja, F. Sichirollo, M. F. da Silva, M. A. Dalla Costa and R. N. do Prado. Reducing storage capacitance in off-line LED power supplies by using integrated converters. IEEE Industry Applications Society Annual Meeting (IAS); 7–11 October 2012; Las Vegas. New York: IEEE; 2012. p.1–8.

[4] D. Camponogara, D. Ribeiro Vargas, M. A. Dalla Costa, J. M. Alonso, J. Garcia and T. Marchesan. Capacitance reduction with an optimized converter connection applied to LED drivers. IEEE Transactions on Industrial Electronics. 2015;**62**:184–192. DOI: 10.1109/TIE.2014.2327591

[5] U.S. Department of Energy. Energy Efficiency Renew. Energy. Lifetime of white LEDs. Pacific Northwest Nat. Lab., Richland, WA, USA, Tech. Rep. 2009.

[6] L. Gu, X. Ruan, M. Xu and K. Yao. Means of eliminating electrolytic capacitor in AC/DC power supplies for LED lightings. IEEE Transactions on Power Electronics. 2009;**24**:1399–1408. DOI: 10.1109/TPEL.2009.2016662

[7] R. Wang, F. Wang, R. Lai, P. Ning, R. Burgos and D. Boroyevich. Study of energy storage capacitor reduction for single phase PWM rectifier. In: Applied Power Electr. Conf., APEC; 15–19 Feb. 2009; Singapore. IEEE; 2009. pp. 1177–1183. DOI: 10.1109/APEC.2009.4802812

[8] F. Zhang, J. Ni and Y. Yu. High power factor AC-DC LED driver with film capacitors. IEEE Transactions on Power Electronics. 2013;**48**(10):4831–4840. DOI: 10.1109/TPEL.2012.2233498

[9] J. C. W. Lam and P. K. Jain. A high power factor, electrolytic capacitor-less AC-input LED driver topology with high frequency pulsating output current. IEEE Transactions on Power Electronics. 2015;**30**(2):943–955. DOI: 10.1109/TPEL.2014.2309555

[10] W. Chen and S. Y. R. Hui. Elimination of an electrolytic capacitor in AC/DC light-emitting diode (LED) driver with high input power factor and constant output current. IEEE Transactions on Power Electronics. 2012;**27**(3):1598–1607. DOI: 10.1109/TPEL.2010.2103959

[11] Y. Wang, J. Huang, W. Wang and D. Xu. A single-stage single-switch LED driver based on Class-E converter. IEEE Transactions on Industry Applications. 2016;**PP**DOI: 10.1109/TIA.2016.2519324,

[12] A. Shrivastava, B. Singh and S. Pal. A novel wall-switched step-dimming concept in LED lighting systems using PFC zeta converter. IEEE Transactions on Industrial Electronics. 2015;**62**:6272–6283. DOI: 10.1109/TIE.2015.2416338

[13] Y. Wang, Y. Guan, K. Ren, W. Wang and D. Xu. A single-stage LED driver based on BCM boost circuit and LLC converter for street lighting system. IEEE Transactions on Industrial Electronics. 2015;**62**:5446–5457. DOI: 10.1109/TIE.2015.2416341

[14] A. Wilkins, J. Veitch and B. Lehman. LED lighting flicker and potential health concerns. In: IEEE Energy Convers. Congr. Expo.; 12 Sep–16 Sep 2010; Atlanta, GA, USA. IEEE; 2010. pp. 171–178.

[15] M. F. de Melo, W. D. Vizzotto, J. M. Alonso and M. A. Dalla Costa. Analysis of series-resonant LED driver applied to reduce the low-frequency current ripple transmission. IEEE 24th International Symposium on Industrial Electronics (ISIE). 2015; pp. 1166–1171.

[16] B. White, H. Wang, Y. Liu and X. Liu. An average current modulation method for single-stage LED drivers with high power factor and zero low-frequency current ripple. IEEE Journal of Emerging and Selected Topics in Power Electronics. 2015;**3**(3). DOI: 10.1109/JESTPE.2015.2424680

[17] S. Whang, X. Ruan, K. Yao, S. C. Tan, Y. Yang and Z. Ye. A flicker free electrolytic capacitor-less AC-DC LED driver. IEEE Transactions on Power Electronics. 2012;**27**(11). DOI: 10.1109/TPEL.2011.2180026

[18] H. Valipour, G. Rezazadeh and M. R. Zolghadri. Flicker-free electrolytic capacitor-less universal input off-line LED driver with PFC. IEEE Transactions on Power Electronics. 2015;**31**(9). DOI: 0.1109/TPEL.2015.2504378

[19] P. S. Almeida, V. C. Bender, H. A. C. Braga, M. A. Dalla Costa, T. B. Marchesan and J. M. Alonso. Static and dynamic photoelectrothermal modeling of LED lamps including low-frequency current ripple effects. IEEE Transactions on Power Electronics. 2015;**30**(7). DOI: 10.1109/TPEL.2014.2340352

[20] C. Park and C. T. Rim. Filter-free AC direct LED driver with unity power factor and low input current THD using binary segmented switched LED strings and linear current regulator. In: Applied Power Electronics Conference and Exposition (APEC); 17 Mar–21 Mar 2013; Long Beach, CA, USA. IEEE; pp. 870–874.

[21] H. Gao, K. Sun, J. Chen, X. Wu, Y. Leng, J. Xi and L. He. An electrolytic-capacitorless and inductorless AC direct LED driver with power compensation. In: Future Energy Electronics Conference; 03 Nov–06 Nov 2013; Department of Electrical Engineering, National Cheng Kung University, Taiwan. IEEE Power Electronics Society; pp. 1–5.

[22] Y. C. Chung, K. M. Lee, H. J. Choe, C. H. Sung and B. Kang. Low-cost drive circuit for AC-direct LED lamps. IEEE Transactions on Power Electronics. 2015;**30**(10). DOI: 10.1109/TPEL.2014.2374160

[23] Texas Instruments. The impact of low frequency ripple current on LEDs and LED drivers' by Texas Instruments at OSRAM Opto Semiconductors and LED drivers' by Texas Instruments at OSRAM Opto Semiconductors [Internet]. Oct. 2010. Available from: http://www.ledlight.osram-os.com/ [Accessed: April 2016].

[24] Lighting Research Center. SSIST: Alliance for solid-state illumination systems and technologies [Internet]. Available from: http://www.lrc.rpi.edu/programs/solidstate/assist/flicker.asp [Accessed: April 2016].

[25] E. Biery. Understand the lighting flicker frustration (magazine) [Internet]. Dec. 2015. Available from: http://www.ledsmagazine.com/ [Accessed: April 2016].

[26] P. D. Teodosescu, M. Bojan and R. Marschalko. Resonant LED driver with inherent constant current and power factor correction. Electronics Letters. 2014;**50**:1087–1088.

[27] P. D. Teodosescu, M. S. Sabau, N. C. Szekely, M. Bojan and R. Marschalko. Electronic device for LED lighting systems. Romanian State Office for Inventions and Trademarks (OSIM). 2015; request no. a 2015 00876.